The Journal of Nutrition
Biochemical, Molecular, and Genetic Mechanisms

Identification of Zyklopen, a New Member of the Vertebrate Multicopper Ferroxidase Family, and Characterization in Rodents and Human Cells[1–3]

Huijun Chen,[4,5,15] Zouhair K. Attieh,[4,6,15] Basharut A. Syed,[4,7] Yien-Ming Kuo,[8] Valerie Stevens,[9] Brie K. Fuqua,[4] Henriette S. Andersen,[9] Claire E. Naylor,[10] Robert W. Evans,[11] Lorraine Gambling,[9] Ruth Danzeisen,[9,12] Mhenia Bacouri-Haidar,[13] Julnar Usta,[14] Chris D. Vulpe,[4]* and Harry J. McArdle[9]

[4]Department of Nutritional Science and Toxicology, University of California, Berkeley, CA 94720; [5]Medical School, Nanjing University, Nanjing 210008, Jiangsu Province, China; [6]Department of Laboratory Science and Technology, American University of Science and Technology, Ashrafieh 1100, Lebanon; [7]Visiongain Ltd, London EC1V 2QY, UK; [8]Department of Medicine, University of California, San Francisco, CA 94143; [9]Rowett Institute of Nutrition and Health, University of Aberdeen, Bucksburn, AB21 9SB, UK; [10]Department of Crystallography, Birkbeck College, London, WC1E 7HX, UK; [11]Division of Biosciences, Centre for Infection, Immunity and Disease Mechanisms, School of Health Sciences and Social Care, Brunel University, Uxbridge, Middlesex, UB8 3PH, UK; [12]International Copper Association, Inc., New York, NY 10016; [13]Department of Biology, Faculty of Sciences, Lebanese University, Hadath 1500, Lebanon; and [14]Department of Biochemistry, School of Medicine, American University of Beirut, Beirut 1103, Lebanon

Abstract

We previously detected a membrane-bound, copper-containing oxidase that may be involved in iron efflux in BeWo cells, a human placental cell line. We have now identified a gene encoding a predicted multicopper ferroxidase (MCF) with a putative C-terminal membrane-spanning sequence and high sequence identity to hephaestin (Heph) and ceruloplasmin (Cp), the other known vertebrate MCF. Molecular modeling revealed conservation of all type I, II, and III copper-binding sites as well as a putative iron-binding site. Protein expression was observed in multiple diverse mouse tissues, including placenta and mammary gland, and the expression pattern was distinct from that of Cp and Heph. The protein possessed ferroxidase activity, and protein levels decreased in cellular copper deficiency. Knockdown with small interfering RNA in BeWo cells indicates that this gene represents the previously detected oxidase. We propose calling this new member of the MCF family "zyklopen." J. Nutr. 140: 1728–1735, 2010.

Introduction

Multicopper ferroxidases (MCF)[16] play a central role in iron nutrition and homeostasis in organisms ranging from yeast to humans (1). The 2 known vertebrate MCF, ceruloplasmin (Cp) and hephaestin (Heph), are hypothesized to facilitate iron transport in diverse tissues by oxidizing ferrous iron to the ferric form, which is subsequently carried by transferrin (2). In these reactions, electrons from 2 ferrous iron are transferred from the MCF type I copper sites to the type II/type III copper site, where molecular oxygen is then reduced to water (3). Without a MCF, the membrane ferrous iron exporter ferroportin 1 (Fpn1) has been shown in some cells to be targeted for degradation, leading to decreased cellular iron efflux (4).

Heph expression is most predominant in intestinal enterocytes and, accordingly, the major phenotype in *sex-linked anemia* mice harboring a mutation in *Heph* is iron deficiency anemia with marked accumulation of iron in the small intestine (5). Heph, however, is also expressed in other tissues, including the brain, pancreas, heart, and lungs (5–8). Cp is mainly found as a soluble serum protein originating from the liver but is also found as a glycosylphosphatidylinositol-linked protein in astrocytes (3). Individuals with mutations in the *Cp* gene (aceruloplasminemia) accumulate iron in multiple tissues, including the liver, pancreas, and brain, leading to diabetes and dementia (9–11). Similarly, targeted disruption of the *Cp* gene in mice results in iron accumulation in multiple tissues (12). Importantly, however, *Cp* null offspring are normal at birth, strongly suggesting that Cp is not essential for iron efflux into the fetal circulation. Similar to hepatic and intestinal iron transport, placental iron transfer from the mother to the fetus requires multiple iron transport steps (13), although the exact mechanisms of placental iron efflux are still not resolved. Ferroxidase-mediated transport, as in other tissues, is a likely scenario but has not yet been characterized.

[1] Supported by NIH grant R01 DK056376 to C.D.V., an NSF Graduate Research Fellowship to B.K.F., a Lebanese University Research Development grant to M.B-H., and a Rural Affairs Research and Analysis Directorate, Scottish Government, EU (EARNEST and NuGO) grant to H.J.M.
[2] Author disclosures: H. Chen, Z. K. Attieh, B. A. Syed, Y-M. Kuo, V. Stevens, B. K. Fuqua, H. S. Andersen, C. E. Naylor, R. W. Evans, L. Gambling, R. Danzeisen, M. Bacouri-Haidar, J. Usta, C. D. Vulpe and H. J. McArdle, no conflicts of interest.
[3] Supplemental Figures 1–4 are available with the online posting of this paper at jn.nutrition.org.
[15] These authors contributed equally to the paper.
[16] Abbreviations used: BCS, bathocuproine disulfonic acid; Cp, ceruloplasmin; E, embryonic (gestation) day; Fpn1, ferroportin 1; GAPDH, glyceraldehyde-3-phosphate dehydrogenase; Heph, hephaestin; MCF, multicopper ferroxidase; pPD, *p*-phenylene-diamine; siRNA, small interfering RNA; SOD1, superoxide dismutase; Zp, zyklopen.
* To whom correspondence should be addressed. E-mail: vulpe@berkeley.edu.

Manuscript received October 22, 2009. Initial review completed January 8, 2010. Revision accepted July 6, 2010.
First published online August 4, 2010; doi:10.3945/jn.109.117531.

We recently identified an endogenous copper-containing oxidase that may play a role in the iron efflux process in placental cells (14). We demonstrated that iron export from BeWo cells, a human trophoblast choriocarcinoma model for placenta, is not enhanced by addition of Cp under a variety of conditions designed to mimic the environment in the fetal circulation. We found no evidence of *Cp* or *Heph* expression using specific cDNA probes in this cell line. Affinity-purified anti-peptide antisera to Heph did not cross-react with any protein in this cell line, but a polyclonal antiserum to the entire Cp protein did detect a cross-reacting protein in BeWo cells (14). We demonstrated that copper deficiency decreases, whereas iron deficiency increases, expression of this protein. Additionally, copper deficiency decreased iron efflux from BeWo cells. From these results, we postulated that an additional multicopper oxidase, distinct from Heph and Cp, is involved in iron export in the placenta (15).

We noted both genomic and expressed sequences in public databases with similar but not identical sequence to Heph and Cp. A GenBank entry listed these sequences under a novel coding sequence termed Hephl1, proposed to encode a multicopper oxidase based on sequence homology to Cp and Heph. In this report, we demonstrate that Hephl1 represents a gene encoding a new member of the multicopper oxidase family most closely related to Heph. We further present evidence that supports our hypothesis that this gene represents the placental MCF, as well as expression data suggesting that this gene plays a role in other tissues as well. We propose that the protein be called "zyklopen" (Zp) after the Zyklops, the mythical one-eyed iron workers in Greek mythology who helped Hephaestus in the forge of the gods.

Materials and Methods

Molecular modeling. Comparative structural modeling of mouse Zp was carried out using Modeler 6.0, a program that satisfies spatial constraints extracted from alignment of target sequences with a template (16,17). Human Cp (Protein Data Bank code 1KCW) (18), which shares 49.4% sequence identity (similarity: 65.6%) with the ectodomain of mouse Zp, was used as the template structure as previously described for modeling of human Heph (19).

Animals and tissue preparation. C57BL6/J mice were obtained from Jackson Laboratory at 6–8 wk of age and fed an AIN-93M diet (20) for 6 wk before being killed, after which tissues were collected. Mice were allowed unlimited access to food and distilled water. All mouse protocols were in accordance with NIH guidelines and approved by the Office of Laboratory Animal Care at the University of California, Berkeley. For immunohistochemistry, adult 10-wk-old ICR (CD-1) mice, fed the diet above from the time of weaning, were purchased from Charles River. The mice were then killed and tissues were processed for immunohistochemistry at the University of California, San Francisco, following approved protocols. When required for mouse studies, timed matings were set up to harvest E [embryonic (gestation) day] 17.5 and E18 embryos and E7 placenta. Female weanling rats of the Rowett Hooded Lister strain were bred at the Rowett Research Institute and killed after mating at E21.5 and placenta was removed for analysis. All rats consumed an AIN-93M diet (20) and distilled water ad libitum and all rat experimental procedures were approved by the Home Office and the Ethics Committee at the Rowett Research Institute and conducted in accordance with the UK Animals (Scientific Procedures) Act, 1986.

Enterocytes were isolated from the multiple cell types of whole intestine, as previously described (21), for subsequent RNA, protein, and activity analyses. Other mouse tissues were homogenized using a Tissue Tearor homogenizer (Cole-Parmer) and cleared by centrifugation (13,000 × *g*; 30 min). Placentas from 21.5-d gestation rats were snap-frozen in liquid nitrogen and then ground with a mortar and pestle to a fine powder.

Cultured cells. BeWo, Caco-2, MCF7, T47D, and MCF10AT cells were obtained from the ATCC (ATCC no. CCL-98, HTB-37, HTB-22, HTB-133, and CRL-10317). BeWo, MCF7, and T47D cells were grown in F12K medium (catalog no. 21127–022, Invitrogen) with 10% fetal bovine serum (Atlanta Biologicals) and 1% penicillin-streptomycin cocktail (Invitrogen) at 37°C in a humidified atmosphere of 95% air 5% CO_2 until 70% confluent. MCF10AT cells were similarly grown, but the medium was supplemented with 0.1 mg/L cholera toxin (Sigma), 10 mg/L insulin (Sigma), 0.5 mg/L hydrocortisone (Sigma), and 0.02 mg/L epidermal growth factor (Invitrogen). Caco-2 cells were grown in DMEM (catalog no. 11960–044, Invitrogen) supplemented with 10% fetal bovine serum, 1% nonessential amino acids (Invitrogen), 1% penicillin-streptomycin cocktail (Invitrogen), and 1% Glutamax (Invitrogen) and harvested at 100% confluency for experiments.

Cell lysis. Cultured cells, mouse tissue homogenates, and enterocytes were washed twice with ice-cold PBS and lysed in PBS containing 1.5% Triton X-100 supplemented with protease inhibitors (catalog no. 1206893, Roche) by passage through a 27-gauge needle. For the rat placenta, ~150 mg of powdered tissue was homogenized in 10 volumes of 20 mmol/L HEPES, 250 mmol/L sucrose, pH 7.4, containing protease inhibitors for 15 s using an Ultra Turrax homogenizing probe on ice. The extracts were centrifuged at 10,000 × *g* for 20 min at 4°C and the supernatants were collected. Protein concentrations were determined using a protein assay kit (BioRad Laboratories).

Total RNA extraction, RT, and PCR. Total RNA was isolated from mouse tissues, BeWo cells, and enterocytes using TRIzol reagent (Invitrogen) according to the manufacturer's protocol. Primers targeting fragments of proposed protein-coding regions of Zp were designed using Primer3 software (22) and ordered from Invitrogen. The sequences (5′-3′) of mouse *Zp* primers were as follows: GGGACATCTGGAAGGAACAA (forward) and CTTTGAAAGTGGCATCAACA (reverse) (954 bp expected product). Human *Zp* primers sequences were AAGATTCAGAAGGAGCCCTA (forward) and CCCAGCATACCAGCTTGTAG (reverse) (672 bp expected product). Three micrograms of total RNA were reverse transcribed using SuperScript II reverse transcriptase (Invitrogen) and oligo-dT primer (Operon). PCR was carried out using *Taq* DNA polymerase as directed by the supplier (Takara). An amplification cycle of 95°C for 45 s, 62°C for 45 s, and 72°C for 2 min was performed in a 100-μL volume. Following 35 cycles, 5 μL of the reaction was removed and the product was separated and visualized on a 1.5% agarose gel containing ethidium bromide. All experiments were repeated independently a minimum of 3 times and representative data are shown.

Antibodies to Zp and other proteins. Rabbit polyclonal antiserum against the unique 15 C-terminal amino acids (AYREVQSCALPTDAL) of Zp was generated and affinity purified (Open Biosystems). Rabbit anti-Heph IgG (raised against QHRQRKLRRNRRSIL) was made previously using the same protocol (21). Cp-specific IgG was from Accurate Chemical and anti-glyceraldehyde-3-phosphate dehydrogenase (GAPDH) IgG was from Chemicon. Peroxidase-labeled anti-mouse and anti-rabbit secondary antibodies were obtained from Santa Cruz Biotechnology and IR-680-conjugated anti-rabbit antibody was from Li-Cor.

Immunoblot analysis. Extracts containing 50 μg protein from rat placenta, mouse tissues, and human cell lines were immunoblotted as described previously (21). Primary antibodies were used at dilutions of 1/1000 for rabbit anti-Zp, 1/2000 for rabbit anti-Heph, and 1:300 for mouse anti-GAPDH. Secondary antibodies were 1/20,000 diluted peroxidase-labeled anti-rabbit or anti-mouse IgG, visualized by enhanced chemiluminescence (Amersham) or 1/20,000 diluted IR680-conjugated anti-rabbit IgG, visualized by an Odyssey imager (Li-Cor). Experiments were repeated independently a minimum of 3 times and representative data are shown.

Immunostaining for Zp in mouse tissue sections. Tissues from ICR (CD-1) 10-wk-old mice and embryos at E17.5 were isolated and fixed for

12–14 h in Bouins fixative (Sigma). Organs were washed in 70% ethanol, dehydrated, embedded in paraffin, and sectioned (8 μm) as previously described (23). Paraffin sections were dewaxed, rehydrated, and steamed for 30 min in 1 mmol/L EDTA followed by treatment with 50 g/L hydrogen peroxide prior to staining. Sections were immunostained using standard procedures with affinity-purified anti-Zp at 1:200 dilution and the VECTASTAIN Elite ABC kit (Vector Laboratories) using the manufacturer's protocol as previously described (24). Staining was visualized with 3,3′-diaminobenzidine (DAB substrate kit, Vector Laboratories) and counterstained with Gills Hematoxylin (Vector Laboratories). Controls included tissues incubated with preimmune serum or anti-Zp serum preadsorbed with 10 μmol/L immunizing peptide for 48 h at 40°C. Sections were examined using a Nikon E800 Eclipse microscope and images captured using a Spot II digital camera. Experiments were repeated independently a minimum of 3 times and representative data are shown.

p-*Phenylene diamine oxidase and ferroxidase activity assays.* Zp *p*-phenylene diamine (pPD) oxidase activity was determined with BeWo cell lysates as previously described (25). Cleared lysates were separated on native nonreducing, nondenaturing 4–12% Tris-glycine PAGE gels (Invitrogen). The gels were then incubated with 0.1% pPD in 0.1 mol/L acetate buffer, pH 5.45, for 2 h and air-dried in the dark. The ferroxidase-specific assay differed from the pPD gel assay only in the final step (25). The gels were placed for 2 h at 37°C in a fresh solution of 0.00784% $Fe(NH_4)_2(SO_4)_2 \cdot 6H_2O$ in 100 mmol/L sodium acetate, pH 5.0. Gels were then washed and rehydrated with 15 mmol/L ferrozine solution in the dark. Color development was then monitored continuously and quantified by scanning densitometry. Purified human Cp (Vital Products) was used as a positive control in both assays. Experiments were repeated independently a minimum of 3 times and representative data are shown.

Small interfering RNA knockdown of Zp *in BeWo cells.* BeWo cells were grown in 6-well plates to 30–40% confluency and then incubated with serum-free DMEM media for 24 h prior to transfection. Cells were then transfected with 160 pmol Stealth Select RNAi small interfering (siRNA) (Invitrogen) set 1 (catalog no. HSS155799, GAGTTTCCTGGCATCTGATTGGATT), set 2 (catalog no. HSS155800, CATCCATTATCATGCTGAGAGCTTT), or set 3 (catalog no. HSS155801, GGTGATGTGATTGTCATTCATTTAA) using Lipofectamine RNAiMAX (Invitrogen) according to the manufacturer's protocol. Cells were harvested 48–72 h post-transfection and then immunoblotted with anti-Zp IgG and assayed for pPD oxidase activity. Immunoblotting of cell extracts with anti-GAPDH IgG was used as a loading control. Experiments were repeated independently a minimum of 3 times and representative data are shown.

Bathocuproine disulfonic acid copper chelation and superoxide dismutase activity assay. BeWo cells (1×10^5) were seeded in 100 mm plates and grown as described. At 70% confluency the medium was supplemented to give final concentrations of 0, 10, 20, 40, 60, 80, and 100 μmol/L bathocuproine disulfonic acid (BCS). After 24 h, cells were harvested by scraping. Superoxide dismutase 1 (SOD1) activity was assayed using a SOD assay kit (Cayman Chemicals) per the manufacturer's instructions, as previously described (25). Briefly, cells were collected by centrifugation at $1000 \times g$ for 10 min at 4°C, lysed, and centrifuged at $1500 \times g$ for 5 min at 4°C. The protein concentration was determined by the Bradford method (BioRad) and then an aliquot of each cell extract was incubated with xanthine oxidase for 20 min and absorbance measured at 450 nm. Duplicate independent experiments to measure SOD1 activity were performed. An aliquot of each extract (30 μg total protein/well) was also examined by immunoblot for Zp and GAPDH. Band intensities were quantified using densitometry with ImageJ (26) and the ratios of each band density to the density of the 0 μmol/L BCS control were multiplied by 100, averaged, and then plotted versus the BCS concentration. Data from 3 independent experiments were analyzed by linear regression analysis using Prism version 5.0 for Macintosh OS X (GraphPad Software).

Results

Identification of Zp. The *zyklopen* gene was initially identified on the basis of sequence homology with *Heph* in the assembly of mouse (XP_146812), rat (XP_235835), and human (XP_291947) whole genome sequences. During the course of this study, Unigene entries under the name *HEPHL1* (Hephaestin-like 1) appeared for mouse (Entrez GeneID 244698) (Mm.325134) and human (Entrez GeneID 341208) (NM_001098672) as well as other species.

Zp has significant sequence similarity with Heph and Cp. The mouse Zp sequence shares 45.9% identity (61.6% similarity) with mouse Cp and 48.8% identity (66.2% similarity) with mouse Heph at the protein level (**Supplemental Fig. 1**). The identity at the nucleotide level is 56 and 59.4%, respectively. Similar to Heph, but distinct from Cp, Zp contains a predicted transmembrane segment near the C terminus. The C-terminal region shares only 23% sequence identity (42.3% similarity) with mouse Heph at the protein level; however, this increases to 47% at the nucleotide level. As can be seen from the sequence alignment, all the residues involved in copper binding and disulfide bond formation in Cp are conserved in Heph and Zp.

Molecular modeling of Zp. Molecular modeling of Zp revealed remarkable structural conservation among Zp, Cp, and Heph (**Fig. 1**). The likely 3D-fold of Zp, like Cp, has 6 domains organized in a triangular array (Fig. 1*B*). Each of the domains exhibits plastocyanin-like folds with β-barrel strands organized in a way reminiscent of the cupredoxin family of redox metalloproteins, which also includes azurin, ascorbate oxidase, and laccase (27). All of the type I, II, and III copper-binding sites for the 6 copper ions in Cp are present in Zp (Fig. 1*C*). Three of the copper ions form the trinuclear metallic unit at the interface of domains 1 and 6. The arrangement closely resembles the one found in the ascorbate oxidase subunit and other structures such as laccases (28,29). The other 3 copper atoms form the mononuclear type I centers and, as in Cp, are organized in domains 2, 4, and 6 (Fig. 1*D*).

Zp and Heph have type I copper centers in domain 2 distinct from Cp. The type I binding sites of blue copper proteins, such as azurin, typically coordinate the copper ion in a distorted tetrahedron or trigonal pyramid arrangement. Three of the ligands (2 histidines and a cysteine) are arranged in a plane around the copper ion and the 4th, a weak and more distal ligand (normally a methionine), forms the pyramid apex. These type I sites are normally seen in Long Range Energy Transfer pathway proteins where the ligand arrangement is an intermediate between that normally seen for Cu^+ (tetrahedron) and Cu^{2+} (distorted Jahn-Teller or square planar), thus facilitating electron transfer by providing a stable environment for both Cu^+ and Cu^{2+}. In human Cp, 2 of the 3 type I centers conform to this typical arrangement (copper 4 and 6 in domains 2 and 4), whereas the 3rd type I site in domain 2 is a tricoordinate copper site lacking the apex methionine, which has been mutated to a nonmetal binding leucine residue in the equivalent position (18,30) (**Supplemental Fig. 2***A*). One of the striking disparities between Zp and Cp, therefore, is the difference in this domain 2 copper-binding site. As is the case with Heph, this site in Zp has the additional methionine residue (M356) that would be able to coordinate the copper ion at this site and thus constitute a typical type I copper environment. In Zp and Heph, the domain 2 binding sites are analogous to the ones in domains 4 and 6 (Supplemental Fig. 2*B*).

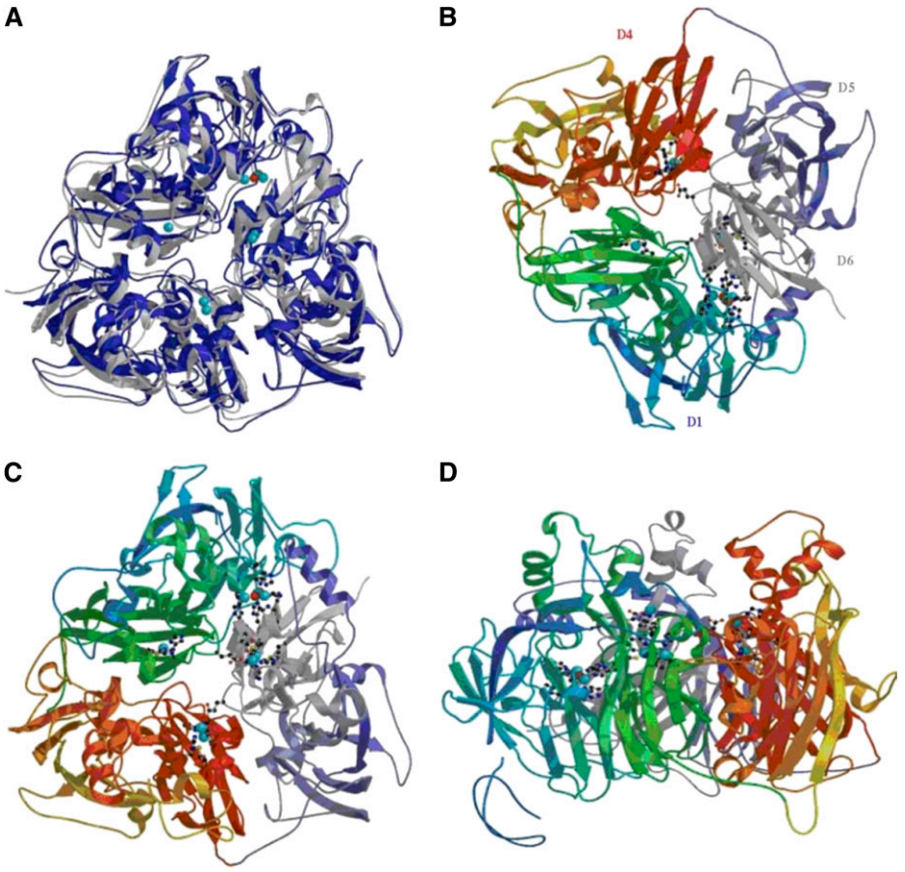

FIGURE 1 Molecular modeling of Zp. (*A*) The superimposition of modeled human Zp on Cp structure. The figures were generated using a modified version of Molscript (43) and subsequently rendered in Raster3D version 2.0 (44). (*B*) The ribbon diagram of Zp shown with top view, bottom view (*C*), and side view (*D*). The residues are colored blue to green for domains 1 and 2 (residues 1–370), yellow to red for domains 3 and 4 (residues 371–720), and lilac to gray for domains 5 and 6 (residues 721–1067). The copper and oxygen atoms are shown in blue and red, respectively.

Zp has a predicted iron binding site. In the Cp structure, additional atypical labile metal ion binding sites were identified close to 2 of the 3 mononuclear sites (Cu 42 and 62) in domains 4 and 6, respectively (31). These may be involved in the ferroxidase activity of Cp. **Supplemental Figure 3** shows the putative iron-binding site of Zp corresponding to the domain 6 labile site in Cp.

Expression of Zp in human BeWo, MCF7, and T47D cells and rodent tissues. PCR amplification of reverse-transcribed RNA from mouse tissues using *Zp*-specific primers demonstrated expression of *Zp* in the heart, kidney, embryo, and, most markedly, the placenta (E7 and E18), but expression was not found in liver or enterocyte (**Fig. 2***A*). A single band was detected for all positive tissues and was of the expected size based on the primer design. Similarly, *Zp* mRNA expression was observed in human BeWo placenta cells (data not shown).

Protein expression of Zp was investigated in rat placenta; mouse serum, enterocyte, embryo, and mammary tissues; and human BeWo, Caco-2, MCF7, T47D, and MCF10AT cell lines.

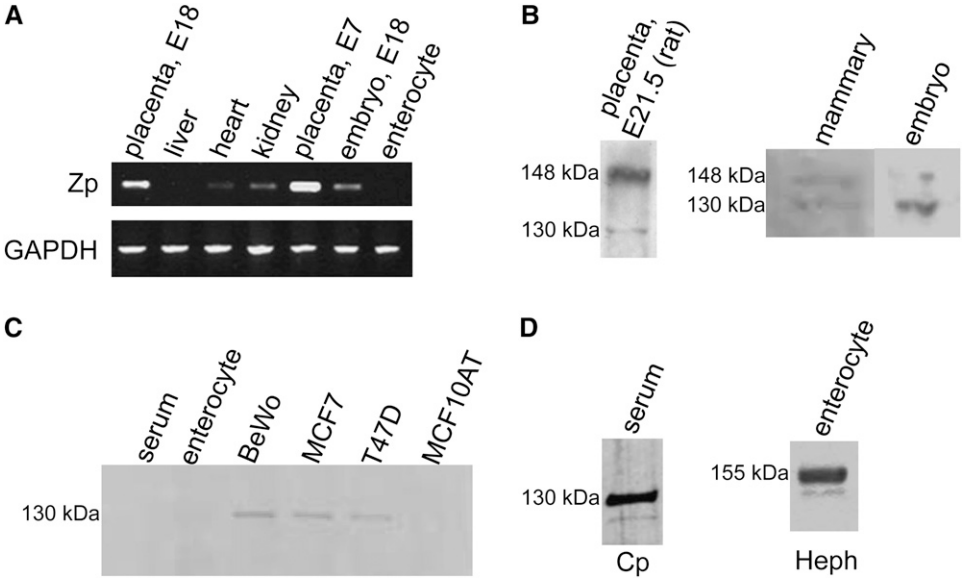

FIGURE 2 Expression of Zp in rodent tissues (*A,B*) and human cell lines (*C*). (*A*) Expression of Zp mRNA in E18 mouse placenta, liver, heart, kidney, E7 placenta, E18 embryo, and enterocytes. GAPDH expression was used as a loading control. (*B*) Immunoblot with Zp-specific IgG of rat placenta, lactating mouse mammary tissue, mouse E18 embryo, and (*C*). mouse serum and enterocytes, and human BeWo, MCF7, T47D, and MCF10AT cell line extracts. (*D*) Immunoblot with Cp- and Heph-specific IgG, respectively, of mouse serum and enterocytes; 50 μg total protein/lane.

Rat placenta immunoreacted with Zp IgG, as well as mouse mammary tissue and whole embryo, revealed a major band at 148 kDa and a minor band at 130 kDa. No signal was observed in mouse serum or enterocytes (Fig. 2*C*) or Caco-2 cell extracts (data not shown) immunoreacted with Zp IgG, indicating that the IgG does not cross-react with Cp or Heph. BeWo, MCF7, and T47D, but not MCF10AT cell extracts, immunoreacted with Zp-specific IgG to give a single band of 130 kDa (Fig. 2*C*). No expression of Cp or Heph was observed in any of these cell lines (data not shown). When samples were immunoreacted with Cp-specific IgG, a major band of 130 kDa was observed in mouse serum (Fig. 2*D*). A single band of 130 kDa was also observed in mammary tissue extracts (data not shown); however, it is not clear if it is circulating Cp or Cp expressed in this tissue.

Immunostaining of Zp in mouse tissues. We examined expression of Zp in mouse adult, embryonic (E17.5), and placental (E15.5) tissues. In the adult, expression was noted in the brain, kidney, testes, and retina (**Fig. 3***A*) but not in the liver or intestine. In the embryo, expression was seen in brain, bladder, eye, and brown fat (Fig. 3*B*). We found expression in placenta in the labyrinth, inverted yolk sac, and spongiotrophoblast (**Supplemental Fig. 4**). This expression pattern is distinct from what has been previously reported for Heph and Cp (3,5–8), although there is coexpression in some tissues, including the

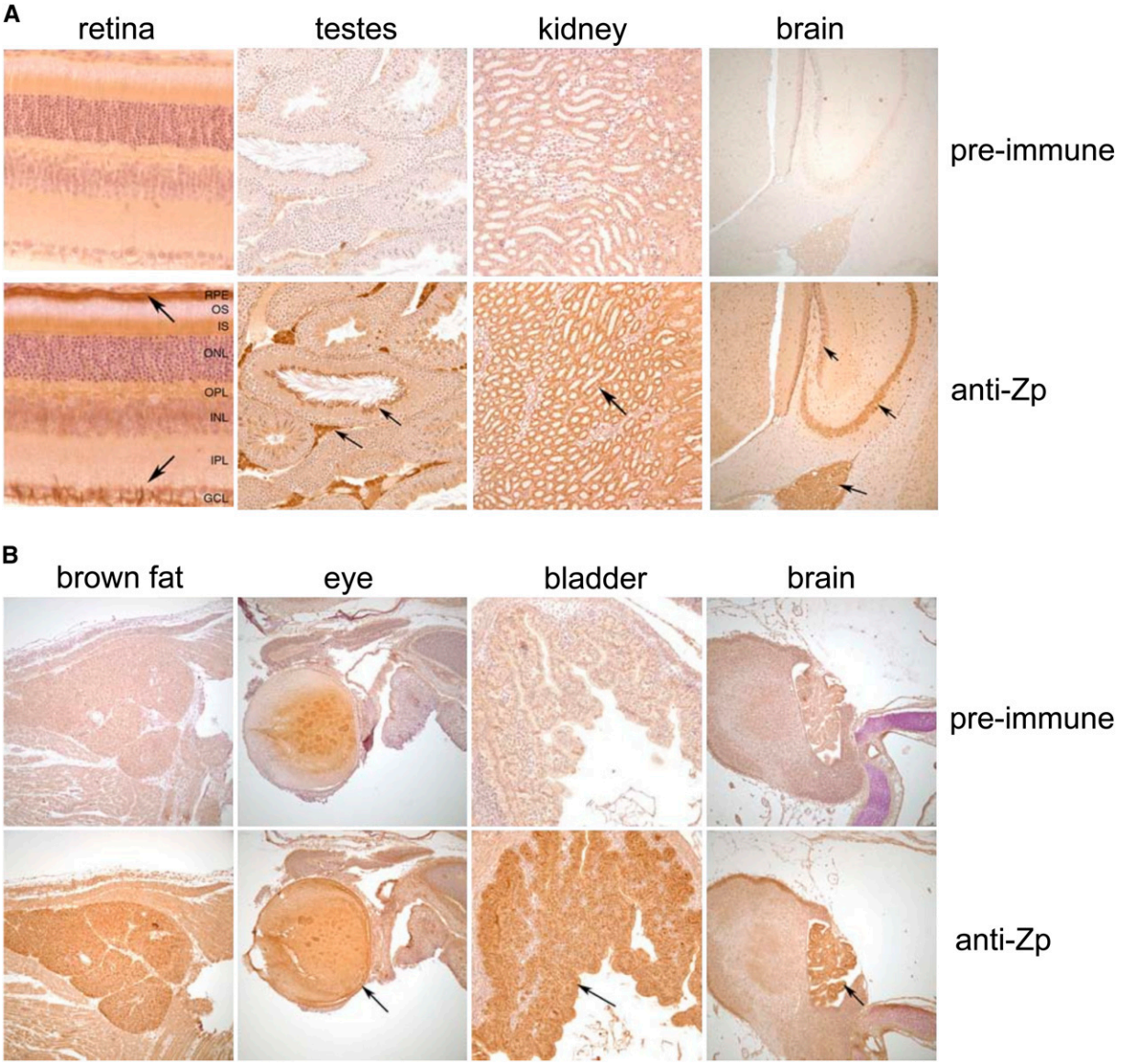

FIGURE 3 Immunostaining of Zp in adult (*A*) and embryonic (*B*) mouse tissues. (*A*) Immunohistochemical localization of Zp in adult mouse brain, kidney, testes, and retina at 10 wk of age. No staining is detected in the preimmune control sera (top row). In the brain, Zp was detected in the choroid plexus, the dentate gyrus, and the CA1 region of the hippocampus (arrow). Zp was localized in cross-sectioned tubules in the kidney medulla and medullary rays (arrow). Zp was highly expressed in the mature spermatozoa of the testes and in the interstitial spaces between the tubules where the endocrine Leydig cells are located (arrow). In the retina, Zp was detected in the retinal pigment epithelium (RPE) and ganglion cell layer (GCL) (arrows). (*B*) Immunohistochemical localization of Zp in embryonic (E17.5) mouse brain, bladder, eye, and brown fat. No staining was detected using the preimmune control sera (top row). Zp expression was high in the choroid plexus of the brain and in the urinary epithelium of the bladder. Zp was also expressed in the E17.5 retina and brown fat. All images were taken at 20× magnification.

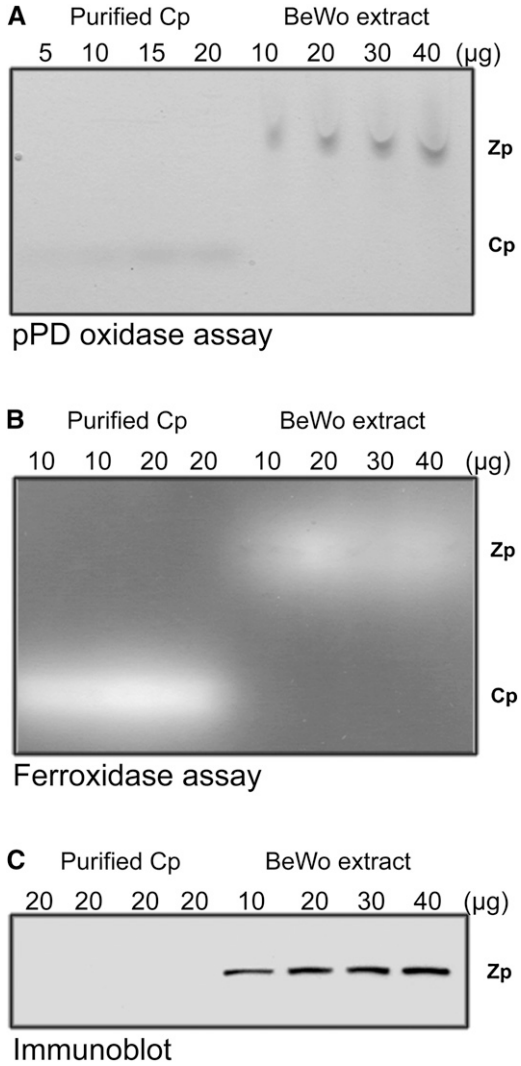

FIGURE 4 pPD oxidase (*A*) and ferroxidase (*B*) activity of Zp in the BeWo human placental cell line. (*A*) In-gel pPD oxidase activity was measured in cell extracts (60, 90, 120, and 150 μg total protein/lane) separated under nondenaturing conditions by native gel electrophoresis. Purified human Cp (5–20 μg/lane) was used as a control. (*B*) In-gel ferroxidase activity of the same extracts in *A*. (*C*) Immunoblot of the same extracts in *A* with Zp-specific IgG.

kidney and placenta (Heph and Zp) and eye and brain (Heph, Cp, and Zp).

Zp has pPD and ferroxidase activities in BeWo cells. Amino acid sequence and homology modeling of Zp with Heph and Cp suggest that Zp has pPD and ferroxidase activities. The pPD and ferroxidase activities of Zp were probed in BeWo cells using in-gel assays and each revealed a single band (**Fig. 4***A*,*B*). The molecular weight of the signal was difficult to assess on the native gels; however, replicate samples immunoreacted with Zp antisera under the same conditions produced a single band comparable in position to that observed in these assays (Fig. 4*C*). BeWo cells do not express Heph or Cp (15).

SiRNA knockdown of Zp *reduces pPD oxidase activity in BeWo cells.* We verified that the signals observed by immunoblot and oxidase assays were Zp by siRNA knockdown of *Zp*. BeWo cells incubated with siRNA primers targeting the *Zp* transcript were immunoblotted and assayed for pPD oxidase

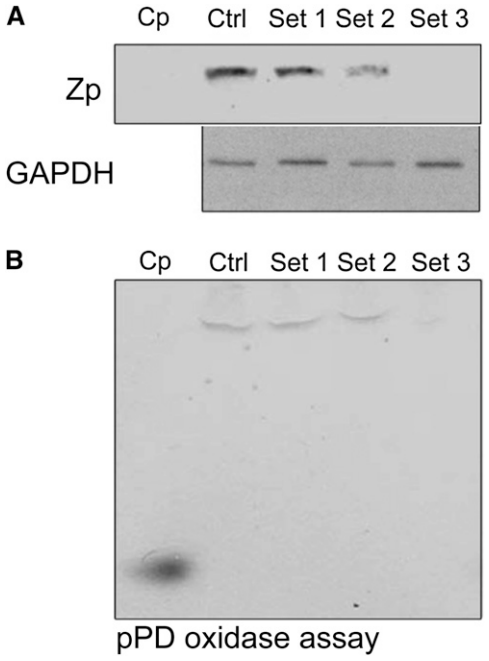

FIGURE 5 pPD oxidase activity in BeWo cells after siRNA knockdown of Zp. (*A*) Immunoblot with Zp- and GAPDH-specific IgG of extracts (100 μg total protein/lane) of nontransfected BeWo cells (Ctrl) and BeWo cells transfected with set 1, set 2, and set 3 siRNA targeting Zp. Purified human Cp was used as a control (20 μg/lane). (*B*) In-gel pPD activity assay of the same samples (100 μg total protein/lane).

activity. Zp protein levels were lower in BeWo cells treated with siRNA primer sets 2 and 3 compared with control (**Fig. 5***A*). Similar results were obtained with the in-gel pPD oxidase activity assay (Fig. 5*B*).

Zp levels are regulated by copper in placental cells. Zp protein levels decreased ($r^2 = 0.926$; $P \leq 0.0005$) in increasingly copper-deficient BeWo cells in parallel with loss of SOD1 activity ($r^2 = 0.982$; $P \leq 0.0001$) (**Fig. 6**).

Discussion

We have identified Zp, a new vertebrate MCF similar to Heph and Cp, which may play a role in placental iron transport. MCF, originally comprising only the serum globulin Cp, now appear to be a family of proteins involved in iron efflux from different tissues. Forty-four vertebrate genomes, as of March 2010, were reported by the Ensembl genome browser to have a protein-coding sequence for Zp (as Hephl1), revealing conservation of this gene. We previously provided physiological data implicating a membrane-bound copper-containing oxidase in the efflux of iron from placental cells. We further demonstrated that the placental oxidase was not Heph, Cp, or their splice variants, although the oxidase showed strong similarities to both (14,15). We now show in this report that Zp represents the previously unidentified placental copper-containing oxidase.

Zp is an MCF based on striking sequence similarity with Heph and Cp, structural modeling, and in-gel ferroxidase assays. All of the type I, II, and III copper-binding sites in Cp are conserved in Zp. In addition, the structural modeling suggests the presence of a putative iron-binding site in domain 6 analogous to sites observed in Cp. In multicopper oxidase blue proteins, substrate binds close to the mononuclear site and

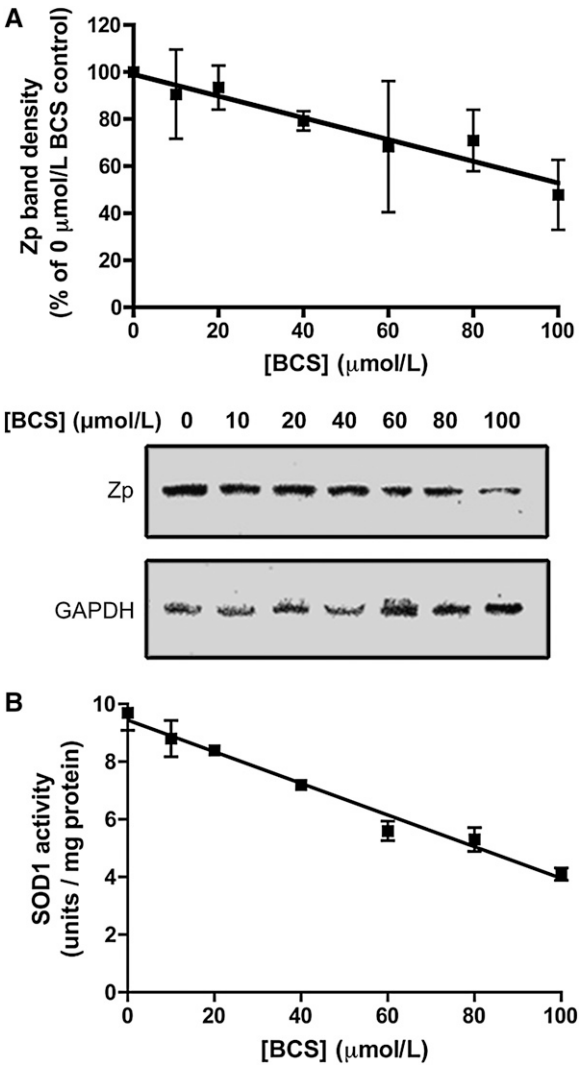

FIGURE 6 Regulation of Zp by copper in BeWo cells. (*A*) BeWo cells were made copper-deficient by incubation with increasing concentrations of BCS, and cell extracts (100 μg total protein/lane) were then immunoblotted with Zp-specific and GAPDH-specific IgG followed by development with chemiluminescence and measurement of band intensity by densitometry. The ratio of each Zp band density to the density of the 0 μmol/L BCS control were multiplied by 100, averaged, and then plotted versus BCS concentration (r^2 = 0.926; $P \leq 0.0005$). Values are means ± SD of results from 3 independent experiments. (*B*) SOD1 activity as measured in the same cell lysates as in *A* and plotted versus BCS concentration (r^2 = 0.982; $P \leq 0.0001$). Values are means ± SD, n = 2 independent experiments.

donates an electron, which is transferred via a cysteine residue to a histidine residue (His-Cys-His motif) involved in binding the trinuclear copper cluster (1). The transfer of electrons through mononuclear copper 6 to the type II and III coppers in the trinuclear cluster would be of primary significance, because molecular oxygen binds to this site and after a transfer of 4 electrons is reduced to 2 molecules of water. These similarities among Zp, Cp, and blue proteins lend strong support for a similar function to Zp. Furthermore, ferroxidase activity in BeWo cells, detected in an in-gel assay, occurred at a comparable position to Zp, as detected by immunoblot. In-gel pPD oxidase activity assay levels also decreased in BeWo cells treated with siRNA against *Zp*, suggesting that this oxidase activity is due to Zp. We also demonstrated decreased protein levels of Zp in cellular copper deficiency as we (25) and others have seen previously for Heph and Cp (3,32,33). The changes in Zp mirror the changes in the protein levels of the unknown placental copper oxidase detected previously (15).

We hypothesize that Zp is a membrane-bound protein involved in iron efflux, perhaps in concert with the iron efflux protein, Fpn1 (34–36). The glycosylphosphatidylinositol-anchored variant of Cp facilitates iron efflux through interaction with Fpn1 (4) and Heph is proposed to actuate iron efflux in a mechanism that likely involves Fpn1 as well (2). Zp is predicted to have a C-terminal membrane-bound region and to have the correct protein topology to interact with Fpn1 with the ferroxidase domain located extracellularly. Fpn1 is expressed in a number of tissues, including placenta (34–37). The ferroxidase-transporter mechanism for iron efflux may therefore be used to transfer iron through the placenta or from the placenta to the fetus via the Zp-mediated conversion of Fe(II) to the Fe(III) form that can be incorporated into fetal transferrin. Our proposed role of Zp in placental iron release is consistent with our own observations (37–39) and those of others (40) that the fetus can maintain iron status despite maternal anemia, but that with copper deficiency, the fetus becomes iron deficient whereas placental iron levels do not decrease. The elucidation of the exact role of Zp in iron efflux in the tissues expressing the gene awaits further experimental work.

The functional role of Zp relative to the other MCF remains unclear. Zp is expressed in a number of tissues, including placenta, but not liver or intestine. We detected 2 bands for Zp in all positive tissues, but not in cell lines, which may represent differences in glycosylation as seen for both Cp and Heph (3,33). Heph is expressed in the placenta as well (8), but the interplay between Heph and Zp in coordinating iron placental egress is not yet known. Zp and Heph could play a similar mechanistic role in mobilization of iron but in distinct placental tissues. Zp could also play a supplemental role in tissues where Cp and/or Heph are also present, perhaps under conditions of unique iron need. In accordance with this, Cp has been shown to augment iron transport from the intestine following severe phlebotomy-induced iron need (41). The 3 MCF may be regulated differently, function in different conditions, or function in different aspects of iron trafficking by certain cells, as is the case for the 2 yeast MCF paralogs Fet3p and Fet5p in *Saccharomyces cerevisiae*, which have distinct yet complementary roles in maintaining cellular iron homeostasis (42). Additional work will be needed to resolve the respective roles of Cp, Heph, and Zp.

Acknowledgments

Z.K.A. designed research; H.C., Z.K.A., B.A.S., Y.M.K., V.S., H.A.S., L.G., and R.D. conducted research; Z.K.A., B.A.S., C.E.N., Y.M.K., B.K.F., and H.J.M. analyzed data and prepared figures; Z.K.A., B.A.S., B.K.F., R.D., M.B-H., J.U., C.D.V., and H.J.M. wrote the paper; and R.W.E. provided intellectual input. All authors read and approved the final manuscript.

Literature Cited

1. Kosman DJ. Fet3p, ceruloplasmin and the role of copper in iron metabolism. Adv Protein Chem. 2002;60:221–69.
2. Anderson GJ, Vulpe CD. Mammalian iron transport. Cell Mol Life Sci. 2009;66:3241–61.
3. Hellman NE, Gitlin JD. Ceruloplasmin metabolism and function. Annu Rev Nutr. 2002;22:439–58.
4. De Domenico I, Ward DM, di Patti MC, Jeong SY, David S, Musci G, Kaplan J. Ferroxidase activity is required for the stability of cell surface

ferroportin in cells expressing GPI-ceruloplasmin. EMBO J. 2007; 26:2823–31.

5. Vulpe CD, Kuo Y-M, Libina N, Askwith C, Murphy TL, Cowley L, Gitschier J, Anderson G. Hephaestin, a ceruloplasmin homologue implicated in intestinal iron transport, is defective in the sla mouse. Nat Genet. 1999;21:195–9.
6. Hudson DM, Curtis SB, Smith VC, Griffiths TA, Wong AY, Scudamore CH, Buchan AM, MacGillivray RT. Human hephaestin expression is not limited to enterocytes of the gastrointestinal tract but is also found in the antrum, the enteric nervous system, and pancreatic beta-cells. Am J Physiol Gastrointest Liver Physiol. 2010;298:G425–32.
7. Hahn P, Qian Y, Dentchev T, Chen L, Beard J, Harris ZL, Dunaief JL. Disruption of ceruloplasmin and hephaestin in mice causes retinal iron overload and retinal degeneration with features of age-related macular degeneration. Proc Natl Acad Sci USA. 2004;101:13850–5.
8. Frazer DM, Vulpe CD, McKie AT, Wilkins SJ, Trinder D, Cleghorn GJ, Anderson GJ. Cloning and gastrointestinal expression of rat hephaestin: relationship to other iron transport proteins. Am J Physiol Gastrointest Liver Physiol. 2001;281:G931–9.
9. Okamoto N, Wada S, Oga T, Kawabata Y, Baba Y, Habu D, Takeda Z, Wada Y. Hereditary ceruloplasmin deficiency with hemosiderosis. Hum Genet. 1996;97:755–8.
10. Takahashi Y, Miyajima H, Shirabe S, Nagataki S, Suenaga A, Gitlin JD. Characterization of a nonsense mutation in the ceruloplasmin gene resulting in diabetes and neurodegenerative disease. Hum Mol Genet. 1996;5:81–4.
11. Yoshida K, Furihata K, Takeda S, Nakamura A, Yamamoto K, Morita H, Hiyamuta S, Ikeda S, Shimizu N, et al. A mutation in the ceruloplasmin gene is associated with systemic hemosiderosis in humans. Nat Genet. 1995;9:267–72.
12. Harris ZL, Durley AP, Man TK, Gitlin JD. Targeted gene disruption reveals an essential role for ceruloplasmin in cellular iron efflux. Proc Natl Acad Sci USA. 1999;96:10812–7.
13. Srai SKS, Bomford A, McArdle HJ. Iron transport across cell membranes: molecular understanding of duodenal and placental iron uptake. Best Pract Res Clin Haematol. 2002;15:243–59.
14. Danzeisen R, Ponnambalam S, Lea RG, Page K, Gambling L, McArdle HJ. The effect of ceruloplasmin on iron release from placental (BeWo) cells: evidence for an endogenous Cu oxidase. Placenta. 2000;21:805–12.
15. Danzeisen R, Fosset C, Chariana Z, Page K, David S, McArdle HJ. Placental ceruloplasmin homolog is regulated by iron and copper and is implicated in iron metabolism. Am J Physiol Cell Physiol. 2002;282:C472–8.
16. Sali A, Blundell TL. Comparative protein modelling by satisfaction of spatial restraints. J Mol Biol. 1993;234:779–815.
17. Fiser A, Do RK, Sali A. Modeling of loops in protein structures. Protein Sci. 2000;9:1753–73.
18. Zaitseva I, Zaitseva V, Card G, Moshkov K, Bax B, Ralph A, Lindley P. The X-ray structure of human serum ceruloplasmin at 3.1 angstrom: nature of the copper centres. J Biol Inorg Chem. 1996;1:15–23.
19. Syed BA, Beaumont NJ, Patel A, Naylor CE, Bayele HK, Joannou CL, Rowe PS, Evans RW, Srai SK. Analysis of the human hephaestin gene and protein: comparative modelling of the N-terminus ecto-domain based upon ceruloplasmin. Protein Eng. 2002;15:205–14.
20. Reeves PG, Nielsen FH, Fahey GC Jr. AIN-93 purified diets for laboratory rodents: final report of the American Institute of Nutrition ad hoc writing committee on the reformulation of the AIN-76A rodent diet. J Nutr. 1993;123:1939–51.
21. Chen H, Su T, Attieh ZK, Fox TC, McKie AT, Anderson GJ, Vulpe CD. Systemic regulation of Hephaestin and Ireg1 revealed in studies of genetic and nutritional iron deficiency. Blood. 2003;102:1893–9.
22. Rozen S, Skaletsky H. Primer3 on the WWW for general users and for biologist programmers. Methods Mol Biol. 2000;132:365–86.
23. Kuo YM, Gitschier J, Packman S. Developmental expression of the mouse mottled and toxic milk genes suggests distinct functions for the Menkes and Wilson disease copper transporters. Hum Mol Genet. 1997;6:1043–9.
24. Kuo YM, Su T, Chen H, Attieh Z, Syed BA, McKie AT, Anderson GJ, Gitschier J, Vulpe CD. Mislocalisation of hephaestin, a multicopper ferroxidase involved in basolateral intestinal iron transport, in the sex linked anaemia mouse. Gut. 2004;53:201–6.
25. Chen H, Huang G, Su T, Gao H, Attieh ZK, McKie AT, Anderson GJ, Vulpe CD. Decreased hephaestin activity in the intestine of copper-deficient mice causes systemic iron deficiency. J Nutr. 2006;136:1236–41.
26. Abramoff MD, Magelhaes PJ, Ram SJ. Image processing with ImageJ. Biophotonics International. 2004;11:36–42.
27. Adman ET. Copper protein structures. Adv Protein Chem. 1991;42: 145–97.
28. Messerschmidt A, Ladenstein R, Huber R, Bolognesi M, Avigliano L, Petruzzelli R, Rossi A, Finazzi-Agro A. Refined crystal structure of ascorbate oxidase at 1.9 A resolution. J Mol Biol. 1992;224: 179–205.
29. Ducros V, Brzozowski AM, Wilson KS, Brown SH, Ostergaard P, Schneider P, Yaver DS, Pedersen AH, Davies GJ. Crystal structure of the type-2 Cu depleted laccase from Coprinus cinereus at 2.2 Å resolution. Nat Struct Biol. 1998;5:310–6.
30. Takahashi N, Ortel TL, Putnam FW. Single-chain structure of human ceruloplasmin: the complete amino acid sequence of the whole molecule. Proc Natl Acad Sci USA. 1984;81:390–4.
31. Zaitsev VN, Zaitseva I, Papiz M, Lindley PF. An X-ray crystallographic study of the binding sites of the azide inhibitor and organic substrates to ceruloplasmin, a multicopper oxidase in the plasma. J Biol Inorg Chem. 1999;4:579–87.
32. Reeves PG, Demars LC, Johnson WT, Lukaski HC. Dietary copper deficiency reduces iron absorption and duodenal enterocyte hephaestin protein in male and female rats. J Nutr. 2005;135:92–8.
33. Nittis T, Gitlin JD. Role of copper in the proteosome-mediated degradation of the multicopper oxidase hephaestin. J Biol Chem. 2004; 279:25696–702.
34. McKie AT, Marciani P, Rolfs A, Brennan K, Wehr K, Barrow D, Miret S, Bomford A, Peters TJ, et al. A novel duodenal iron-regulated transporter, IREG1, implicated in the basolateral transfer of iron to the circulation. Mol Cell. 2000;5:299–309.
35. Donovan A, Brownlie A, Zhou Y, Shepard J, Pratt SJ, Moynihan J, Paw BH, Drejer A, Barut B, et al. Positional cloning of zebrafish ferroportin1 identifies a conserved vertebrate iron exporter. Nature. 2000;403: 776–81.
36. Abboud S, Haile DJ. A novel mammalian iron-regulated protein involved in intracellular iron metabolism. J Biol Chem. 2000;275: 19906–12.
37. Gambling L, Danzeisen R, Gair S, Lea RG, Charania Z, Solanky N, Joory KD, Srai SK, McArdle HJ. Effect of iron deficiency on placental transfer of iron and expression of iron transport proteins in vivo and in vitro. Biochem J. 2001;356:883–9.
38. Andersen HS, Gambling L, Holtrop G, McArdle HJ. Effect of dietary copper deficiency on iron metabolism in the pregnant rat. Br J Nutr. 2007;97:239–46.
39. McArdle HJ, Andersen HS, Jones H, Gambling L. Fetal programming: causes and consequences as revealed by studies of dietary manipulation in rats: a review. Placenta. 2006;27:S56–60.
40. Ervasti M, Sankilampi U, Heinonen S, Punnonen K. Early signs of maternal iron deficiency do not influence the iron status of the newborn, but are associated with higher infant birthweight. Acta Obstet Gynecol Scand. 2009;88:83–90.
41. Cherukuri S, Potla R, Sarkar J, Nurko S, Harris ZL, Fox PL. Unexpected role of ceruloplasmin in intestinal iron absorption. Cell Metab. 2005;2:309–19.
42. Spizzo T, Byersdorfer C, Duesterhoeft S, Eide D. The yeast FET5 gene encodes a FET3-related multicopper oxidase implicated in iron transport. Mol Gen Genet. 1997;256:547–56.
43. Esnouf RM. Polyalanine reconstruction from Calpha positions using the program CALPHA can aid initial phasing of data by molecular replacement procedures. Acta Crystallogr D Biol Crystallogr. 1997;53: 665–72.
44. Merritt EA, Murphy ME. Raster3D version 2.0. A program for photorealistic molecular graphics. Acta Crystallogr D Biol Crystallogr. 1994;50:869–73.